PHYSICAL REVIEW A VOLUME 40, NUMBER 9 NOVEMBER 1, 1989

Entanglements in random systems

Yacov Kantor
School of Physics and Astronomy, Tel Aviv University, Tel Aviv 69978, Israel

Gregory N. Hassold
Department of Materials Science and Engineering, University of Michigan, Ann Arbor, Michigan 48109-2136
(Received 5 July 1989)

Topological entanglements play an important role in the physical properties, such as viscosity, of macromolecular structures. We investigate the likelihood of the appearance of entanglements in the bond percolation problem. We show that *below* the percolation threshold p_c (but extremely close to it) there exists an entanglement threshold p_e. Between p_e and p_c, there exists an infinite spanning group of interlocked (linked) clusters. Thus, in a strong gelation process, the sol-gel transition appears at p_e rather than at p_c. We define the problem and discuss the possible approaches to its resolution. We apply the Monte Carlo renormalization-group approach to find the distance between the thresholds, and investigate some numerical characteristics of the entangled clusters. The achieved numerical resolution of $p_c - p_e \approx 2.3 \times 10^{-7}$ required averaging over an extremely large numbers of configurations.

I. INTRODUCTION

An important problem of the statistical mechanics of macromolecules is how to account for topological entanglements. At experimentally relevant temperatures, most of the polymers are unbreakable, and, therefore, two segments of the same or different polymers are prevented from crossing each other during their motion in a solvent. In its simplest form the effect of entanglements can be demonstrated by the physics of a solution of ring polymers, which behaves differently from a solution of linear polymers of the same length, since a pair of such rings created separately is prevented from interpenetrating by topological constraints, while a pair of rings which have been created in an interlocked (linked) state cannot be separated without breaking up the macromolecules. Topologically interlocked rings, denoted "catenanes" in the chemical literature, are common in many polymeric materials.[1,2] Even for a single-ring molecule, the topological entanglements play an important role since the phase space of all possible configurations splits into several subspaces, each corresponding to a different knot type. A molecule in a particular knotted state cannot access configurations corresponding to a different knot. Clearly, the constraints strongly influence both the static and dynamic properties of polymers. One should, however, clearly separate the *topological* entanglements, affecting the equilibrium thermodynamics, from the *dynamical* "entanglement constraints,"[3] which slow down the relaxation processes in polymers even in the absence of true topological entanglements.

The problem of entanglements was first clearly formulated by Delbrük[4] and since received a considerable attention. Usually, calculation of thermodynamic functions involves integrations over all possible states of a system, which disregards the fact that the phase space may be split into several mutually inaccessible regions. Since the correct physics of the system must take into account the fact that the initial conditions limit the accessible phase space, one must supplement the purely Hamiltonian description of the problem, by constraints which would impose that limit.[5] Usually, macromolecular systems fluctuate very strongly, and their behavior is primarily determined by their *connectivity* and the excluded volume (or steric) interactions. Thus, their properties are determined by the available phase space, i.e., by the entropy S. In particular, the elasticity of rubbers and gels is, predominantly, of entropic origin.[6] Since the introduction of topological constraints severely reduces S, it has a major effect on the properties of entropy-dominated systems.[7] Attempts to incorporate the topological entanglements into the theory of rubber elasticity were pioneered by Deam and Edwards,[8] and, by a somewhat different approach, by Graesley and Pearson.[9] More recently, Iwata developed a formalism[10] which can be conveniently applied to regular (periodic) networks. Even in such simple systems, the treatment involves numerous approximations. The randomness of the crosslinking in dense systems can be accounted for by means of the replica method.[11,12]

In the gel-formation process[13] a solution of short chains (sol) is chemically crosslinked to form clusters of increasing size. The increase in the concentration p of crosslinks leads to increased viscosity η. At a certain concentration p_g (gelation threshold) the viscosity diverges, and the system starts behaving as a solid (gel). Just below p_g, the viscosity $\eta \sim (p_g - p)^{-s}$. Above p_g, the (entropic) elastic stiffness increases with increasing p. Close to the threshold, the shear modulus μ can be described by a power law $(p - p_g)^t$. The gelation process can be modeled by a percolation problem,[14] in which p is the fraction of present bonds or sites on a regular lattice. While such modeling oversimplifies the actual geometry of the growing clusters,[15] it is frequently used due to the

conceptual simplicity representing the generic disordered system. The gelation threshold p_g is usually identified with the percolation threshold p_c, at which an infinite cluster (or a single macromolecule spanning the entire solid) appears. Such an approach envisions a gel just above p_g as an infinite cluster and many finite clusters, as depicted in Fig. 1(a). Physical characteristics of the transition, such as the entropic elasticity of the gel,[16] are usually analyzed under this assumption.

However, the viscosity of a solution of macromolecules may be infinite (while the shear modulus may be finite) *even in the absence of a single molecule spanning the entire system,* since it suffices to have a spanning group of interlocked (linked) molecules to produce that effect. Such behavior would appear in the "Olympic state" of a system of interlocked ring molecules, suggested by de Gennes.[13] Such a system, depicted in Fig. 1(b), can be created artificially. However, much more interesting is to find out whether the entanglements are frequent in completely random systems. If this is true, the gelation threshold p_g will be smaller than p_c, and the geometry of the gel just above p_g will be represented by Fig. 1(c).

In this work we investigate the role played by entanglements in random systems by analyzing a standard three-dimensional percolation problem. We set aside the question of elasticity, and focus our attention on the geometrical and topological aspects of the problem. We show that below the usual percolation threshold p_c, there exists a distinct *entanglement threshold* p_e, which should be identified with p_g of the gelation process. Some of our results have already been published.[17] In this paper, we both present the previously published results, which have been improved by an increased statistics, as well as include new information related to the geometrical features of entangled clusters, and shortly overview the possible approaches to the problem and provide details of our method of calculation. Section II defines the problem and overviews the available theoretical tools for its treatment. Section III describes the finite-size scaling approach to the problem, as well as presents the details of the numerical algorithm, and discusses the problems and prospects of larger scale simulations. In Sec. IV we present the results of the numerical simulations: We show that $\Delta p_{ce} \equiv p_c - p_e$ *does not vanish,* and describe some quantitative characteristics of entangled clusters. Finally in Sec. V, we discuss the possible theoretical extensions of the work, as well as applicability of the results to experimental systems.

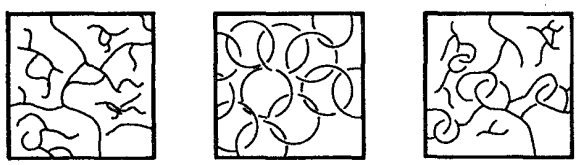

FIG. 1. Schematic drawing of several solid systems having finite entropic elastic constants: (a) system with a percolating (infinite) cluster; (b) infinite cluster of entangled (yet not connected) ring polymers; (c) random system with an infinite cluster formed by entangled *finite* macromolecules.

II. ENTANGLEMENTS IN RANDOM SYSTEMS—CONCEPTS AND APPROACHES

The main object of the mathematical theories of topological entanglements is the developing of mathematical methods for link and knot detection and discrimination. While the existence of knots is an intuitively obvious fact, the rigorous proofs of existence and effective methods of knot detection date back only to 1920s, while the investigation of the influence of entanglements on the physical properties of the systems started in the 1960s. In a general space dimension d one can distinguish many types of topological entanglements. We will be concerned with the case of two or more entangled loops (link), such as depicted in Figs. 1(b)–1(e). Such entanglement of *linear* objects is possible only in $d=3$. However, one may also consider more general kinds of entanglements, such as a closed loop surrounding a *point* in $d=2$, or a surface encapsulating a point in $d=3$, or entanglements between a line and a surface in $d=4$. Some properties of entanglements of higher-dimensional manifolds have been investigated by Duplantier.[18] Since we are interested in the behavior of macromolecular structures, we shall remain in the realm of entanglements between linear objects.

There exist numerous methods of link detection: The simplest approach detects the presence of a topological link between two loops l_1 and l_2 by calculating the Gaussian invariant:[19]

$$\mathcal{L}_{12}=\frac{1}{4\pi}\oint_{l_1}\oint_{l_2}\frac{(d\mathbf{r}_1\times d\mathbf{r}_2)\cdot(\mathbf{r}_1-\mathbf{r}_2)}{|\mathbf{r}_1-\mathbf{r}_2|^3}\ . \tag{2.1}$$

If the (integer) result of this double integration does not vanish, the loops are linked. $\mathcal{L}_{12}$ measures the number of times one loop crosses through the other: It vanishes for the nonentangled configuration depicted in Fig. 2(a) and is equal to ± 1 (the sign depends on the choice of direction of integration) for a simple entanglement of two loops depicted in Fig. 2(b) and is equal to ± 2 for a more complicated entanglement depicted in Fig. 2(c). The simplicity of the invariant (2.1) leads to its extensive use in the analytical treatment of the entanglement problem.[7,20,21] The numerical evaluation of $\mathcal{L}_{12}$ does not involve a calculation of continuous line integrals, since it can be reduced to intersection counting on the projections of the loops on an arbitrary plane,[22] and, therefore, can be efficiently used in numerical simulations.

Unfortunately, $\mathcal{L}_{12}$ does not discriminate well between different kinds of links. In particular, there exist entangled (linked) configurations, such as depicted in Fig. 2(d), for which $\mathcal{L}_{12}$ vanishes.[23] It also cannot be used to investigate self-entanglements of a single loop (knot).[24] A significantly better resolution of knots and links can be obtained by the use of Alexander polynomials.[25] However, the construction of those polynomials is defined algorithmically, thus preventing their use in analytical treatments, and restricting their application to numerical investigations.[23,24] Alexander polynomials are unable to resolve several different (very complicated) knots and

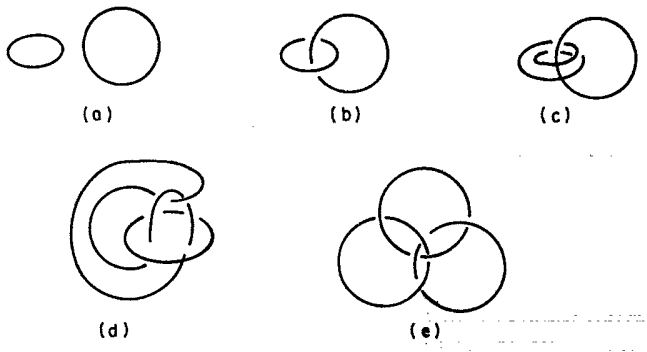

FIG. 2. Examples of linked loops: (a) trivial, unlinked case with $\mathcal{L}=0$; (b) simple link with $\mathcal{L}=1$; (c) simple link with $\mathcal{L}=2$; (d) nontrivial link with $\mathcal{L}=0$; (e) triplet of entangled rings (Borromean rings) which are *not* pairwise entangled.

links.[26] However, from the practical point of view they are sufficiently discriminative for most problems. Recently, even more powerful invariants have been found,[27] however, they had not yet been implemented in the calculation of the properties of physical systems.

In a regular percolation problem a pair of bonds belongs to the same *connectivity* cluster if there is a continuous path of present bonds connecting them. If the probability p for bonds to be present exceeds the threshold value p_c, an infinite connectivity cluster is present in the system. We will say that two bonds belong to the same entanglement cluster if they either belong to the same connectivity cluster, *or* belong to different connectivity clusters which cannot be separated without violating the topological constraints. One should keep in mind that entanglement is a global property, which cannot be detected by a simple inspection of the local environment of each bond. Moreover, one might have a situation, resembling Borromean rings, where a triplet of connectivity clusters is entangled, while each pair of that triplet, viewed separately, is not entangled [see Fig. 2(e)]. Our primary goal is to find the entanglement threshold p_e, above which there exists an infinite entanglement cluster. From the definitions it is clear that $p_e \leq p_c$; the main purpose of our work was the establishment of the strict inequality $p_e < p_c$. Near the threshold, the behavior of the system should be described by a set of critical exponents analogous to the regular percolation problem: The root-mean-squared size of a finite entanglement cluster, denoted as correlation length ξ_e, is expected to diverge as $|p-p_e|^{-\nu_e}$, while above the threshold, the volume fraction of the infinite entanglement cluster should be described by a power law $(p-p_e)^{\beta_e}$. Similarly, one can define other critical exponents.

One should bear in mind a formulation of the same question in terms of plaquette percolation:[28] Consider a dual of the bond percolation problem, in which we place a plaquette in the middle of each absent bond, perpendicular to it. The concentration of the plaquettes will be $q=1-p$. One can easily understand the meaning of the threshold value $q_c=1-p_c$ by considering a large finite system: If the bonds do not percolate in, say, the vertical direction, one can find a collection of plaquettes forming an *orientable* surface separating the system into upper and lower parts. Thus the threshold q_c signifies the appearance of an infinite orientable surface in the system. This surface will not, in general, be *simply connected.* Moreover, if $p_e < p_c$, then in the range $q_c < q < q_e = 1-p_e$ all infinite surfaces will have handles. The threshold q_e will therefore signify the appearance of the first infinite simply connected surface.

As in the regular percolation, one may try a variety of approaches to the problem in question. However, one quickly discovers that certain techniques used in regular percolation are almost useless in the entanglement problem. For example, series expansions[29] can hardly be used for these purposes: The smallest possible pair of entangled clusters in a three-dimensional bond percolation problem on a cubic lattice consists of two square loops of size 2×2. Since the number of bonds in such a configuration is 16, the differences between the regular and entanglement percolations in the low-concentration p expansions will appear at the order p^{16}. (In the site percolation on the same lattice the differences will appear at the order p^{32}.) One can hardly imagine using ϵ-expansion-type techniques (for determination of the critical exponents), since it is not clear what is the proper generalization of the problem to an arbitrary space dimensionality, and because a satisfactory treatment should involve constraints (such as Alexander polynomials) which have no convenient representation. So, at this early stage of the investigation of entanglements, we are left with the possibility of the numerical investigation, which, as we shall see in the following sections, is by itself on the "borderline" of what can been done with today's computing means.

III. THE NUMERICAL PROCEDURE

The quantitative analysis of the problem relies on the finite-size scaling, or large-cell Monte Carlo renormalization-group[30] method: In the case of a regular percolation problem we define a contact probability $X_c(p,L)$ that a finite $L\times L\times L$ system percolates in, say, the z direction. We may treat $X_c(p,L)$ as the renormalized probability of a bond to be present after the original problem has been rescaled by a factor L. The fixed point $p^*(L)$ of such renormalization-group transformation is determined from the equation $X_c(p^*,L)=p^*$, and provides an estimate of p_c, since $\lim_{L\to\infty} p^*=p_c$. Actually, the equation defining the fixed point has three solutions, and we disregard two of them, $p^*=0$ and $p^*=1$, which represent the trivial (stable) fixed points. In an infinite system, the root-mean-squared size of a finite connectivity cluster, called the correlation length ξ_c, diverges as p approaches p_c: $\xi_c=a|p-p_c|^{-\nu_c}$, where $\nu_c\approx0.9$ for the three-dimensional percolation,[14] while the prefactor a is of order unity. Far away from the percolation threshold, where $\xi_c < L$, we have $X_c\approx0$ ($X_c\approx1$) for $p<p_c$ ($p>p_c$). Thus, the width of the region in which X_c increases from 0 to 1 is of order L^{-1/ν_c}, and the slope

$$\alpha(L)\equiv\left[\frac{\partial X_c}{\partial p}\right]\Bigg|_{p=p^*}\sim L^{1/\nu_c}\ . \tag{3.1}$$

Actually, this relation can be used to define the exponent ν_c:

$$\nu_c\equiv\lim_{L\to\infty}\frac{\ln L}{\ln\alpha(L)}\ . \tag{3.2}$$

It is worthwhile to note that in the range of L's used in our simulations ($L\sim 10$), we expect to have a slope $\alpha(L)\sim 10$.

Similarly, we can define a probability $X_e(p,L)$ that the system is entangled (i.e., either percolates *or* cannot be separated into two parts without violating the constraints) in the z direction, and use this function to obtain an estimate $p_e^*(L)$ of the entanglement threshold p_e as well as the value of the critical exponent ν_e characterizing the correlation length ξ_e. *A priori,* there is no reason to expect equality between ν_c and ν_e. Therefore, *for sufficiently large* L, the slopes of X_c and of X_e at their respective fixed points may be different. One can easily see that the expected distance between the estimates of the critical points $\Delta p_{ce}^*\equiv p^*-p_e^*$ is extremely small: The smallest possible entangled configuration on a cubic lattice consists of two interpenetrating (but not touching) loops of sizes 2×2 each. This minimal configuration consists of 16 bonds, and its probability for $p\approx\frac{1}{4}$ will be smaller than $p^{16}\sim 10^{-10}$. In the simulation we used boundary conditions in which the entire boundary layer consisted of present bonds, as depicted in Figs. 4–6. Figure 3 depicts the smallest possible entanglement on $L=3$ lattice. For $L\le 2$ entangled configurations are impossible, while for $L\sim 10$ we expect to have very small Δp_{ce}^*. (The numerical simulations indeed show that $\Delta p_{ce}^*\sim 10^{-8}$–$10^{-7}$ in the relevant range of L's.) Since $X_e\ge X_c$, and both curves are smooth, for $L\sim 10$ they are well approximated by straight lines in a range of p's satisfying $|p-p^*|<0.1$. This range of linear behavior by many orders of magnitude exceeds Δp_{ce}^*. Therefore, we conclude that *for values of L relevant to our simulation* the slopes of X_c and X_e *coincide,* and in the vicinity of p^* they are well approximated by two parallel straight lines. Thus, instead of measuring Δp_{ce}^*, we can measure the quantity

$$\begin{aligned}\Delta X&\equiv X_e(p^*,L)-X_c(p^*,L)\\&=X_e(p_e^*,L)+(\partial X_e/\partial p)\Delta p_{ce}^*-X_c(p^*,L)\\&=(\alpha-1)\Delta p_{ce}^*\ .\end{aligned}$$

Since $\alpha\sim 10$ in the relevant range, the quantity ΔX is

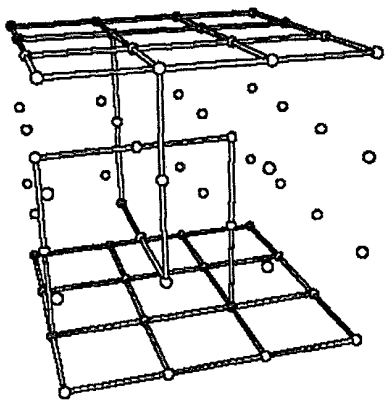

FIG. 3. Smallest possible entangled configuration on $L=3$ lattice. The spheres represent the lattice sites, and the cylinders represent the relevant bonds. The z axis has been chosen as the direction of percolation and/or entanglement. The boundary conditions used in the simulation are evident in the filling of the top and bottom planes with bonds.

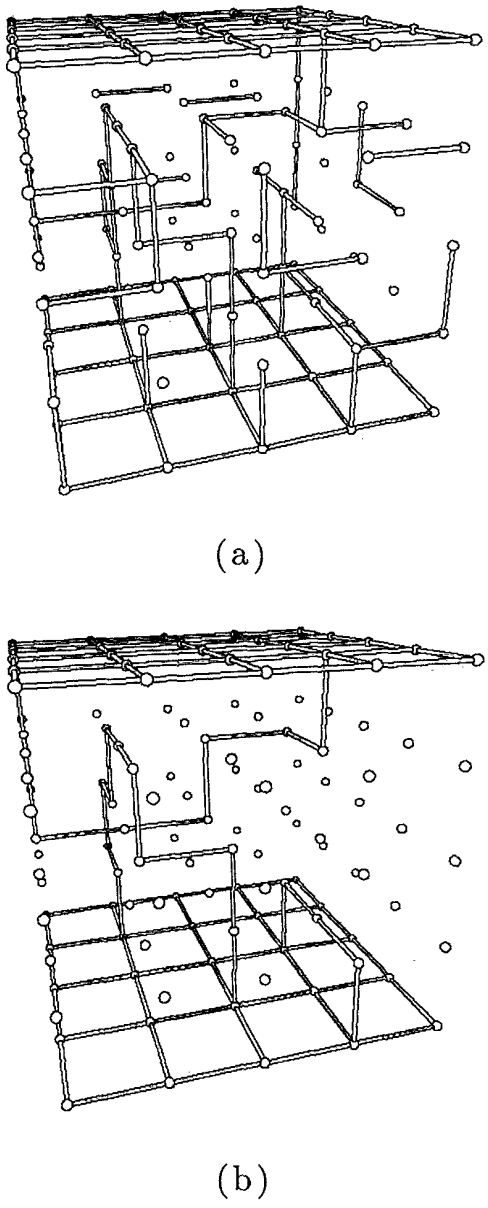

FIG. 4. Typical entangled nonpercolating configuration for $L=4$. (a) The original random configuration. (b) The same configuration after all small loops and dangling bonds (without large loops) have been removed. Boundaries are filled with present bonds, and increase the probability of loop occurrence.

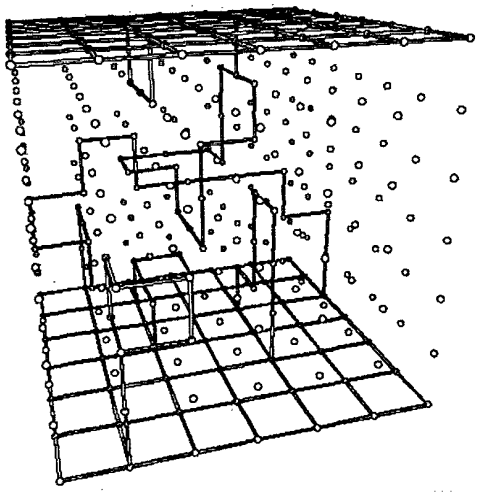

FIG. 5. Typical entangled nonpercolating configuration for $L=6$, "shaved" from dangling bonds and small loops. The entanglement appears "in the middle of the lattice" without the assistance of the boundary conditions.

larger than Δp_{ce}^* by an order of magnitude, and, therefore, more easily measurable. ΔX is just the probability of finding *a nonpercolating, yet entangled* realization for given L and p.

We considered lattices with $L=4$, 6, 12, and 18. On those lattices we examined 192, 40, 10, and 6 *millions* of configurations, respectively. The total simulation consumed eight months of CPU time on an Apollo DN 3000 and Sun 4/110ME minicomputers. (The most time consuming parts of the algorithm are not vectorizable, and an attempt to execute the programs on a Cyber 205 supercomputer gained only an 18-fold increase in speed.) Since the program demanded relatively small memory, but required enormous execution times, the large redundancy of the data structure has been used to accelerate the calculation.

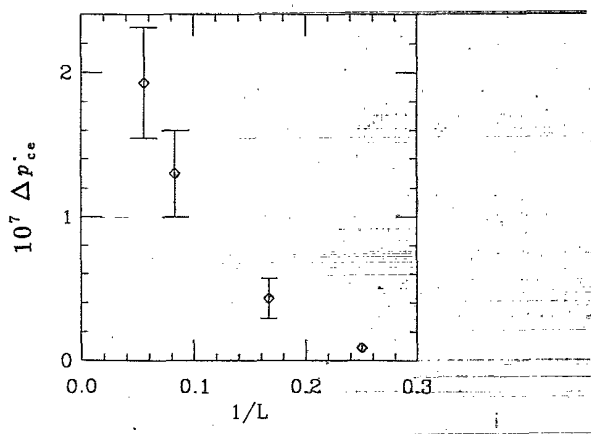

FIG. 6. Successive distances between the fixed points Δp_{ce}^* as a function of inverse cell size $1/L$. Error bars are the estimated standard deviations due to the finite number of realizations. The extrapolation of the graph to $1/L=0$ (as indicated by the arrow) gives the distance between the percolation and entanglement thresholds.

The first stage of the analysis of a randomly generated sample consisted of removal of small loops (consisting of four bonds) and "shaving" of the clusters from dangling ends, which do not contain large loops. (However, care had to be taken not to destroy large loops in the small-loop elimination process.) We also removed all clusters which were not connected to either upper or lower boundaries of the lattice. (Neglect of those clusters is justified below.) This process significantly simplifies the following treatment of the configurations. Figure 4 depicts a typical entangled configuration for $L=6$ before and after the "shaving." The numerical advantage of removal of the clusters not connected to the boundaries and of removal of approximately half of the bonds in the clusters which are attached to the boundaries is self-evident.

At the next stage, the remaining loops have been found using an algorithm based on the "burning" method:[31] One bond of the cluster (e.g., a bond on the boundary of a lattice) is chosen to be "burned" at the zeroth time step. At the nth time step one burns all present previously "unburned" bonds which are adjacent to bonds burned in the $(n-1)$th time step. Two simultaneously "burned" bonds emerging from the same site identify a branching point, and the site is denoted as a "root." Each "burned" bond has a pointer indicating its predecessor in the burning process, as well as an indicator of the last "root" which appeared on the way towards the present "burning." Two simultaneously "burned" bonds, entering the same site, close a loop, which can be found by tracing back the latest common "root" of both bonds, and by creating a complete list of bonds belonging to that loop with the use of "backwards pointers." (The redundant use of "backwards pointers" and "root indicators" accelerates the loop-detection process.) Only loops containing eight bonds or more are registered, since smaller loops cannot create an entanglement. The final stage of the procedure consists of testing for entanglements between pairs of loops belonging to different connectivity clusters: First we check whether the loops are located in the vicinity of each other, and if they are indeed sufficiently close, we calculate the Gaussian invariant (2.1) by projecting the loops on a plane, and analyzing the intersections of the projections.[22] This could be, in principle, the most time consuming process, since the link detection between two loops consisting of L_1 and L_2 bonds requires L_1L_2 operations. However, the elimination of small loops and the test whether two loops are sufficiently close to each other eliminate the need for most of the calculations of the Gaussian invariant.

It is interesting to observe the influence of the boundary conditions on the formation of entanglements: For $L=3$ case, depicted in Fig. 3, the presence of the boundary layer is crucial for the possibility of appearance of an entanglement. In the $L=4$ case, a significant part of the bonds in the loops which form the entanglement still belongs to the boundaries. Thus, in these cases, a particular choice of boundaries provides a significant assistance to the formation of entanglements. However, in the $L=6$ case, depicted in Fig. 5, the entanglement already appears without the assistance of the boundaries.

Simulations were performed at $p^*(L)$. Note, that despite the small value of Δp_{ce}^*, the wide range over which X_c and X_e are linear permits us to use a low-accuracy value for p^*. Thus, we were able to determine *difference* in the thresholds with accuracy of order 10^{-7}, while the locations of the fixed points were known only up to three-digit accuracy. One should keep in mind that ΔX is extremely small in the considered range of L's, and therefore, it sufficed to examine only "direct" entanglements between the loops belonging to the cluster attached to the upper boundary of the lattice and the loops belonging to the cluster attached to the lower boundary—the probability of entanglement via an intermediate cluster is completely negligible. We mentioned in the previous section that the Gaussian invariant may not detect certain entangled configurations. Thus, in principle, this method of calculation would only establish a lower bound on ΔX. However, even the simplest entangled configuration with vanishing $\mathcal{L}_{12}$ with topology depicted in Fig. 2(d) contains at least 34 bonds, and in the relevant range of L's, the probability of occurrence of such a link is completely negligible (and many orders of magnitude below the accuracy of our calculation). For similar reasons, we can neglect the possibility of appearance of "nonpairwise" entanglements, such as Borromean rings. Thus, within the accuracy of our results, we obtain the actual value of ΔX, rather than its lower bound.

In the following section we will show, that, in order to investigate the *critical* exponents of the entanglement problem, L must exceed 300. In principle for very large L's ($L \gg 100$), below p_c, the number of loops should increase as the volume of the system, and, therefore, the number of operations required to examine a single configuration should increase as L^6. In the intermediate range of L's (say, $L \sim 50$), where one still can neglect the entanglements via intermediate clusters, only the "semi-infinite" connectivity clusters attached to the opposite boundaries are relevant, and we expect the number of operations to increase as L^{2D}, where D is the fractal dimension[32] of the "shaved" connectivity cluster. (Probably, it coincides with the fractal dimension of the entire cluster, i.e., it is ≈ 2.5.) However, in the range of our simulation $L \sim 10$, the time increased only as L^3, since the time consumption was not yet dominated by the checks of entanglements between the pairs of loops. The increase in time is partially compensated by the increase of entanglement probability, and the time per entangled configuration increased very slowly, reaching 80 h CPU for $L = 18$ (on Apollo DN 3000). We estimate that there will be a need for, at least, few *months* of CPU time per *single* entangled configuration in the interesting range of $L \sim 300$, where one should expect to see a clear separation between p_c and p_e. Moreover, one should keep in mind that for large cells one will need more elaborate methods of link detection, and entanglements between a pair of connectivity clusters "mediated" by an additional cluster will also play an important role. Thus, unless an efficient vectorizable algorithm for entanglement detection can be found, one can hardly expect to investigate the critical exponents of the entanglement problem in the near future.

IV. POSITION OF p_e AND PROPERTIES OF ENTANGLEMENT CLUSTERS

Among the millions of examined configurations for each L only $n \sim 10$–25 entangled nonpercolating configurations were found. Under these conditions, the appearance of entangled configurations is governed by the Poisson process, and the estimated statistical error is just $\sqrt{n}$. Thus, the accuracy of our estimates of ΔX and Δp_{ce}^* is only about 20% to 30%. [Since, the slope α is known to better than 1% accuracy, it does not further contribute to the uncertainty of $\Delta p_{ce}^*(L)$.] Figure 6 depicts the sequence of estimates $\Delta p_{ce}^*(L)$ as a function of $1/L$. The estimated asymptotic value is $\Delta p_{ce} \approx 2.3 \times 10^{-7}$. Notice, an upwards curvature of the entire curve: One may suspect that the actual value of Δp_{ce} is somewhat larger than the value quoted above. (This curvature was not so pronounced in the previously published results[17] due to their lower accuracy.) While the distance between the critical points is very small, there is not much doubt that it is finite.

Since we are still quite far away from a reliable scaling regime it is quite difficult to predict the exact dependence of the entanglement probability on L. However, if we assume an approximate power-law dependence, then from our data we may estimate that for $L \approx 300$ most of nonpercolating configurations at p^* will be entangled.

The extreme closeness of two critical points prevents investigation of the critical properties of entanglement clusters near $p = p_e$ for such small cells. We, nevertheless, measured several quantitative characteristics of the entangled configurations. It has been noted by Coniglio[33] that a percolating configuration at p_c on a finite lattice is comprised from several multiply connected regions, which are interconnected by one-dimensional segments of singly connected (or "red") bonds, the destruction of which would disconnect the lattice. He has further shown that the average number L_r of "red" bonds is proportional to L^{ν_c}. It can also be shown that in a disconnected configuration, there exist singly disconnecting (or "pink") bonds, such that reconnection of any one of them will create a percolating cluster. The number of "pink" bonds L_p (Ref. 34) is also proportional to L^{ν_c}. Thus the measurement of L_r and L_p can be used to evaluate ν_c. The arguments used in establishing those relations in the regular percolation problem can be directly implemented for the entanglement problem: In a (large) finite lattice at p_e the role of the "red" bonds is played by the bonds, whose removal will "disentangle" the system. The number L_c of such "singly disentangling" bonds (continuing the color nomenclature, we denote them "crimson" bonds) should increase with the lattice size as L^{ν_e}. Figure 7 depicts on a logarithmic scale the L dependence of L_c, measured only for the nonpercolating, yet entangled configurations. Were this measurement to be performed for very large L, where most of the configurations are entangled, its slope would provide us with the value of ν_e. The numbers of "crimson" bonds by an order of magnitude exceed the L_r in the percolating configurations, i.e., the configurations are "very fragile" and can be disentan-

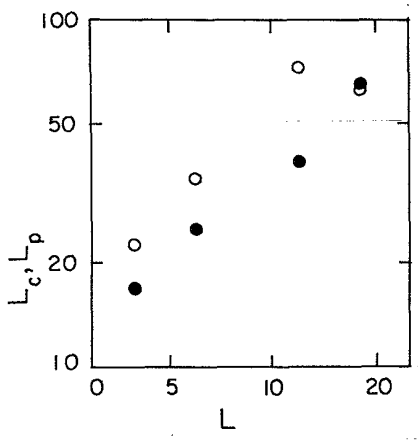

FIG. 7. Logarithmic plot of numbers of "pink" (L_p) and "crimson" (L_c) bonds (see text) in entangled nonpercolating configurations as a function of lattice size L at $p = p^*(L)$.

gled by breaking a single bond in many places. On the other hand, the slope of the curve is approximately 1, i.e., is consistent with the value of ν for a regular percolation. However, one should not forget that we are not in the desired large-L regime, i.e., the entangled configurations are exceptional, and the entire data collected on the entangled configuration has a negligible contribution to the general averages, due to rarity of the entangled configurations.

The equivalent of the "pink" bonds in the percolation problem, should be the bonds, whose addition creates an entangled or percolating configuration. (However, since p_e is strictly lower than p_c, for sufficiently large L it is impossible to create a percolating configuration by an addition of single bond at $p = p_e$.) We *did not* measure the numbers of those "singly entangling" bonds. The measurement of L_p which is relevant only to the percolation problem (see Fig. 7), again indicates a slope close to 1, and the values of L_p significantly larger than those in regular (not entangled) nonpercolating samples. This result, again confirms our claim that the shape of the entangled samples is rather exceptional. The fractal dimension of the entangled nonpercolating cluster has been measured and appears to be consistent with the fractal dimension of regular percolation.

So far the quantitative data on the (exceptional) entangled configurations does not show any pronounced differences between the regular percolation and the entanglement problem. If, indeed the only difference between the two problems consists in the fact that small loops in neighboring connectivity clusters are occasionally entangled, this would mean that the entanglement problem is essentially equivalent to percolation problem with a somewhat shifted p_c. However, this is all one can expect to see on such small lattices. On the other hand, the nonlocal nature of the entanglement constraint, and the possibility of entanglements consisting of more than a single pair of loops, lead to the expectation that the critical properties at p_e will be different from those of the connectivity clusters at p_c. The discrete nature of *lattice* percolation requires the presence of rather large loops (i.e., being close enough to p_c) before entanglements become physically possible. In lattices with large coordination numbers (e.g., the simple cubic lattice with nearest-neighbor and next-nearest-neighbor connections) one may have rather small entangled loops. However, the increase in the coordination number decreases the p_c, and it does not seem to be possible to further separate the critical points. One might consider further investigation of the critical properties near p_e using percolating systems with short-range correlations.

V. DISCUSSION

It is interesting to observe that the presented problem is specifically *three-dimensional*—it has no two-dimensional analog. It is unclear whether objects of larger topological dimension, which are able to create entanglements, appear in higher-dimensional percolation problems, and what is the proper generalization of this problem to an arbitrary dimension.

Viscosity and entropic elasticity of gels depend on both connectivity and entanglements, and therefore can only be used to determine the position of p_e. If one wants to distinguish between the two thresholds experimentally, one needs to perform an additional measurement of a quantity which is insensitive to entanglements. In principle, one should be able to establish the position of p_c by measuring the p dependence of the *energetic* elasticity, which is created by bond-stretching and bending forces in a gel. This type of elasticity originates in the energy (U) part of the free energy $F = U - TS$ and is independent of the temperature T. Energetic elastic constants vanish at p_c with a large critical exponent,[35] which differs from the critical exponent of entropic elasticity, which disappears at p_e. In an ideal system it should be possible to separate the energetic and entropic contributions from the measurements of the T dependence of the elastic moduli, and, thus determine the difference between p_c and p_e. Unfortunately, additional temperature-dependent effects will probably prevent such separation.

The entanglements may appear to be important even in the physical systems, where p_e is practically indistinguishable from p_c, since their relative importance will increase as p_c is approached from above. An important future avenue of research should be investigation of the changes in the *physical* properties of random systems in the presence of entanglements.

ACKNOWLEDGMENTS

We thank M. V. Jarić and M. Kardar for numerous discussions, and for their continuous interest in the problem. It is a pleasure to acknowledge discussions with B. I. Halperin, D. R. Nelson, L. Peliti, L. Schulman, and D. Vanderbilt on various aspects of this problem. This work was supported by the Foundation for Basic Research at Tel Aviv University and by Bat-Sheva de Rothschild Foundation.

[1]G. Schill, Catenanes, *Rotaxanes and Knots* (Academic, New York, 1971).

[2]H. L. Frisch and E. Wasserman, J. Am. Chem. Soc. **83**, 3786 (1961), and references therein; see, also, R. Wolovsky, *ibid.* **92**, 2132 (1970); D. A. Ben-Efraim, C. Batich, and E. Wasserman, *ibid.* **92**, 2133 (1970); J. C. Wang, Acc. Chem. Res. **6**, 252 (1973).

[3]W. W. Graesley, Adv. Poly. Sci. **16**, 1 (1974), and references therein; M. Doi and S. F. Edwards, *The Theory of Polymer Dynamics* (Clarendon, Oxford, 1986), and references therein.

[4]M. Delbrük, in *Mathematical Problems in Biological Sciences,* edited by R. E. Bellman [Proc. Symp. Appl. Math. **14**, 55 (1962)].

[5]S. F. Edwards, Proc. Phys. Soc. **91**, 513 (1967).

[6]For recent review see S. F. Edwards and Th. Vilgis, Rep. Prog. Phys. **51**, 243 (1988), and references therein.

[7]S. F. Edwards, J. Phys. A **1**, 15 (1968).

[8]T. Deam and S. F. Edwards, Philos. Trans. R. Soc. London Ser. A: **280**, 317 (1976).

[9]W. W. Greasley and D. S. Pearson, J. Chem. Phys. **66**, 3363 (1976).

[10]K. Iwata, J. Chem. Phys. **76**, 6363 (1985); **76**, 6375 (1985).

[11]R. C. Ball and S. F. Edwards, Macromol. **13**, 748 (1980).

[12]P. M. Goldbart and N. G. Goldenfeld, Phys. Rev. Lett. **58**, 2676 (1987); Phys. Rev. A **39**, 1402 (1989); **39**, 1412 (1989).

[13]See, e.g., P. G. de Gennes, *Scaling Concepts in Polymer Physics* (Cornell University Press, Ithaca, New York, 1979).

[14]D. Stauffer, *Introduction to Percolation Theory* (Taylor and Francis, London, 1985).

[15]For review, see H. J. Herrmann, Phys. Rep. **136**, 155 (1986).

[16]See, e.g., D. Stauffer, A. Coniglio, and M. Adam, Adv. Poly. Sci. **44**, 103 (1982).

[17]Y. Kantor and G. N. Hassold, Phys. Rev. Lett. **60**, 1457 (1988).

[18]B. Duplantier, Commun. Math. Phys. **85**, 221 (1982).

[19]P. Alexandroff and H. Hopf, *Topologie I* (Springer, Berlin, 1935).

[20]F. W. Wiegel, in *Phase Transitions,* edited by C. Domb and J. L. Leibowitz (Academic, London, 1983), Vol. 5, p. 101; *Introduction to Path-Integral Methods in Polymer Science* (World Scientific, Singapore, 1986), and references therein.

[21]M. G. Brereton and S. Shah, J. Phys. A **13**, 2751 (1980); **14**, L51 (1981); **15**, 985 (1982).

[22]See, e.g., R. Ball and L. Mehta, J. Phys. **42**, 1193 (1981).

[23]A. V. Vologodskiĭ, A. V. Lukashin, and M. D. Frank-Kamenetskiĭ, Zh. Eksp. Teor. Fiz. **67**, 1875 (1974) [Sov. Phys.—JETP **40**, 932 (1975)].

[24]A. V. Vologodskiĭ, A. V. Lukashin, M. D. Frank-Kamenetskiĭ, and V. V. Anshelevich, Zh. Eksp. Teor. Fiz. **66**, 2153 (1974) [Sov. Phys.—JETP, **39**, 1059 (1974)].

[25]See, e.g., R. H. Crowell and R. H. Fox, *Introduction to Knot Theory* (Ginn, Boston, 1963).

[26]See, e.g., J. H. Conway, in *Computational Problems in Abstract Algebra,* edited by J. Leech (Pergamon, Oxford, 1970), p. 329.

[27]P. Freyd, D. Yetter, J. Hoste, W. B. R. Lickorish, K. C. Millet, and A. Ocneanu, Bull. Am. Math. Soc. **12**, 239 (1985).

[28]M. Aizenman, J. T. Chayes, L. Chayes, J. Frölich, and L. Russo, Commun. Math. Phys. **92**, 19 (1983); J. Kertész and H. J. Herrmann, J. Phys. A **18**, L1109 (1985).

[29]J. W. Essam, Rep. Prog. Phys. **43**, 833 (1980), and references therein; D. S. Gaunt and M. Sykes, J. Phys. A **16**, 783 (1983), and references therein.

[30]P. J. Reynolds, W. Klein, and H. E. Stanley, J. Phys. C **10**, L167 (1977); P. J. Reynolds, H. E. Stanley, and W. Klein, Phys. Rev. B **21**, 1223 (1980).

[31]H. J. Herrmann, D. C. Hong, and H. E. Stanley, J. Phys. A **17**, L261 (1984).

[32]B. B. Mandelbrot, *Fractals: Form Chance and Dimension* (Freeman, San Francisco, 1977); *The Fractal Geometry of Nature* (Freeman, San Francisco, 1982).

[33]A. Coniglio, J. Phys. A **15**, 3829 (1982).

[34]A. Coniglio, in *Physics of Finely Divided Matter,* edited by N. Boccara and M. Daoud (Springer, Berlin, 1985); for detailed derivation, see D. C. Wright, D. J. Bergman, and Y. Kantor, Phys. Rev. B **33**, 396 (1986).

[35]Y. Kantor and I. Webman, Phys. Rev. Lett. **52**, 1891 (1984).